Absorption cross sections, kinetics of formation, and self-reaction of the IO radical produced via the laser photolysis of N2O/I2/N2 mixtures

ARTICLE *in* THE JOURNAL OF PHYSICAL CHEMISTRY · JULY 1995

Impact Factor: 2.78 · DOI: 10.1021/j100030a013

3 AUTHORS, INCLUDING:

Michael J. Kurylo
Universities Space Research Association
184 PUBLICATIONS **6,267** CITATIONS
SEE PROFILE

Robert Huie
National Institute of Standards and Technology
192 PUBLICATIONS **7,935** CITATIONS
SEE PROFILE

Absorption Cross Sections, Kinetics of Formation, and Self-Reaction of the IO Radical Produced via the Laser Photolysis of $N_2O/I_2/N_2$ Mixtures

Barna Laszlo, Michael J. Kurylo, and Robert E. Huie*

Chemical Kinetics & Thermodynamics Division, National Institute of Standards & Technology, Gaithersburg, Maryland 20899

Received: March 2, 1995; In Final Form: May 22, 1995[⊗]

The laser photolytic production of the IO radical from $N_2O/I_2/N_2$ mixtures was used to measure the radical absorption spectrum from 340 to 450 nm. Two new absorption peaks at 403 and 411 nm were observed along with an underlying continuum starting at about 420 nm and extending to about 350 nm. An absorption cross section of $(2.8 \pm 0.5) \times 10^{-17}$ cm^2, in good agreement with previous measurements, was determined for the (4−0) band head at 427.2 nm. From the rate of formation of IO and the rate of loss of I_2, rate constants for the reactions $O + I_2 \rightarrow IO + I$ and $O + IO \rightarrow O_2 + I$ of $(1.4 \pm 0.4) \times 10^{-10}$ and $(1.2 \pm 0.5) \times 10^{-10}$ cm^3 s^{-1}, respectively, were derived. Finally, from the rate of decay of IO, a rate constant for the reaction $IO + IO \rightarrow$ products of $(8.0 \pm 1.8) \times 10^{-11}$ cm^3 s^{-1} was obtained. All of the uncertainties expressed are 2 standard deviations derived from the statistical analysis and do not include estimates for possible systematic errors.

Introduction

The proposed role of iodine-containing species in the chemistry of the troposphere has been discussed by a number of authors.[1−6] This role has been described by two sets of reactions whose principal effect appears to be that of altering the speciation within certain chemical families such as NO_x. Both reaction sets are initiated by the reaction of the iodine atom with ozone.

$$I + O_3 \rightarrow IO + O_2 \quad (1)$$

Since I atoms do not readily abstract hydrogen from saturated organic compounds nor readily add to unsaturated compounds, this appears to be their major tropospheric reaction. Because of its long-wavelength absorption, the product IO undergoes rapid photolysis.

$$IO + h\nu \rightarrow I + O \quad (2)$$

The resulting oxygen atoms will react with molecular oxygen to reform ozone.

$$O + O_2 \rightarrow O_3 \quad (3)$$

Alternatively, the IO may react with NO to form NO_2,

$$IO + NO \rightarrow I + NO_2 \quad (4)$$

which is then readily photolyzed to return O atoms and thence O_3.

A number of nonactive reservoir iodine species can also be formed in the troposphere. The most important are HOI, formed in the reaction

$$IO + HO_2 \rightarrow HOI + O_2 \quad (5)$$

and $IONO_2$, formed in the reaction

$$IO + NO_2 \rightarrow IONO_2 \quad (6)$$

Steady-state concentrations of these species, along with the radicals I and IO, have been calculated for various NO_x concentrations.[5] It is the repeated formation of such reservoir compounds, followed by their conversion to IO_x species, that can influence the abundance of tropospheric ozone.[6,7]

By analogy with the better-known chlorine and bromine cycles,[7] iodine is expected to participate in several sets of catalytic reactions leading to the destruction of stratospheric ozone. This possibility has recently been reviewed by Solomon et al.[8,9] The simplest cycle involves reaction 1 followed by either

$$IO + O_3 \rightarrow I + 2O_2 \quad (7)$$

or

$$IO + O \rightarrow I + O_2 \quad (8)$$

In the catalytic sequence of reactions 1 and 7, reaction 7 is quite slow ($k_7 < 1.2 \times 10^{-15}$ cm^3 s^{-1} at 292 K[10]) and is the rate-limiting process. While reaction 8 can be expected to occur with a rate constant many orders of magnitude greater, its role, like that of the corresponding reaction in the Cl system, is limited to the upper stratosphere, where the abundance of O atoms is largest. The photolysis of IO, however, may also play an important role in limiting the direct catalytic effect of iodine in stratospheric ozone depletion.

IO can also undergo self-reaction:[11]

$$IO + IO \rightarrow 2I + O_2, \Delta H = -47 \text{ kJ mol}^{-1} \quad (9a)$$

$$\rightarrow I + OIO \quad (9b)$$

$$\rightarrow I_2 + O_2, \Delta H = -198 \text{ kJ mol}^{-1} \quad (9c)$$

(The thermodynamic values used in these and subsequent calculations are from Stein et al.[12] except for $\Delta H_f = 130$ kJ mol^{-1} for IO, which was estimated previously.[13]) The role of this reaction in regenerating atomic iodine in the stratosphere is probably quite small due to the relatively low concentration of IO throughout the atmosphere. It is, however, important in laboratory investigations of other reactions of IO, particularly

[⊗] Abstract published in *Advance ACS Abstracts,* July 1, 1995.

its reactions with ClO and BrO. Just as the reaction between ClO and BrO plays a very important role as a chain-carrying step in catalytic ozone loss throughout the polar and midlatitude stratosphere, the reactions of IO with ClO and BrO must also be considered.[8,9] These reactions may lead to the regeneration of halogen atoms and merit strong consideration in explaining ozone losses observed in the midlatitude lower stratosphere.

$$IO + ClO \rightarrow I + Cl + O_2, \Delta H = -4 \text{ kJ mol}^{-1} \quad (10a)$$

$$\rightarrow I + ClOO, \Delta H = -28 \text{ kJ mol}^{-1} \quad (10b)$$

$$\rightarrow I + OClO, \Delta H = -29 \text{ kJ mol}^{-1} \quad (10c)$$

$$\rightarrow ICl + O_2, \Delta H = -214 \text{ kJ mol}^{-1} \quad (10d)$$

$$IO + BrO \rightarrow I + Br + O_2, \Delta H = -37 \text{ kJ mol}^{-1} \quad (11a)$$

$$\rightarrow I + BrOO, \Delta H = -40 \text{ kJ mol}^{-1} \quad (11b)$$

$$\rightarrow I + OBrO, \Delta H = -19 \text{ kJ mol}^{-1} \quad (11c)$$

$$\rightarrow IBr + O_2, \Delta H = -215 \text{ kJ mol}^{-1} \quad (11d)$$

It is important to note that the reaction channels producing two halogen atoms are exothermic, unlike the reactions of ClO with itself and with BrO, for which such a channel is endothermic. It is also significant that the channels producing ICl or IBr are the most exothermic and are equivalent to the atom formation channels due to the rapid photolysis of both ICl and IBr in sunlight. The formation of thermally unstable products such as ClOO and BrOO also result in atom regeneration and ozone loss. Only the formation of OClO and OBrO result in a null cycle if their photodissociation leads to O + ClO (or BrO). Thus, it is likely that atomic halogen formation reaction channels will be more significant in reactions 10 and 11 than in the reactions ClO + ClO and ClO + BrO. To date, however, there is very little published data on the reaction rates for the various IO reactions that are likely to be important in describing the role of iodine chemistry in stratospheric ozone loss. Therefore, we have initiated the investigation of various iodine monoxide reactions of atmospheric importance. In this paper, we report on our results on the absorption spectrum of IO, the rate constants for the reactions O + I_2 and O + IO, and the kinetics of the self-reaction of IO. Of the three reactions, O + IO is of greatest atmospheric importance. The other two are significant for characterizing the photochemical kinetic experiments in the studies of the inter-halogen reactions that we are presently conducting.

Experimental Section

Apparatus and Procedure.[14] The experiments were carried out employing laser photolysis followed by kinetic absorption spectrophotometry. The apparatus is diagrammed in Figure 1. Light from the 75-W Hamamatsu xenon arc analysis lamp is rendered nearly parallel using an Aspherab condenser and two long-focal-length lenses. The light passes end-on through a 5-cm diameter, 10-cm-long cylindrical quartz cell. The light traverses the cell twice, is deflected by a prism, and is divided by a 50/50 beam splitter. Each half of the analysis beam is focused on the slit of a monochromator. The first, a Kratos GM 252 monochromator with a 2365 grooves/mm grating, blazed at 300 nm, was typically operated with a slit width of 0.2 mm, yielding a resolution of 0.3 nm. This monochromator

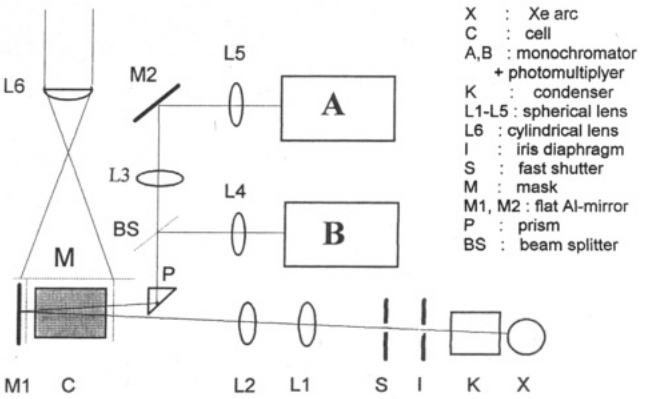

Figure 1. Schematic diagram of optical arrangement.

was used to monitor the IO radical and to measure its spectrum. The second, an Oriel 77250 1/8 m monochromator with a 1200 grooves/mm grating was usually set at 530 nm with 2-nm bandwidth to monitor I_2. In a few of the later experiments, this monochromator was replaced with a Jobin Yvon H25 with an 1800 grooves/mm grating.

The output of a Questek Model 2320 excimer laser was expanded by a cylindrical lens and filled the cell side-on through a 2 × 10 cm Suprasil flat with minimal variation in light intensity over the cell length. The magnitude of this variation was established by photolyzing 400 Torr (53 kPa) O_2 while masking all but 1-cm-wide regions of the window and monitoring the amount of O_3 formed. The photolytic light intensity showed a Gaussian-like profile with an approximately 20% difference between the maximum and minimum values. Computer modeling revealed that this results in less than a 2% error in the calculated second-order rate constants. For all of the experiments reported here, the laser was operated at 193 nm, using ArF as the fill gas.

For many of the experiments, a fast shutter was located between the xenon lamp and the reaction cell to reduce the extent of photolysis by the analyzing light. There was no apparent effect on the kinetic results. Cutoff filters also were employed before the reaction cell. Electronic signals from two Hamamatsu R955 side-on photomultipliers were fed into a Tektronix 7612D two-channel, multitimebase waveform digitizer through a Tektronix 7A13 differential comparator (Kratos) and a 7A22 differential amplifier (Oriel). In later experiments, two 7A13 comparators were used. In the absence of a transient absorber, the voltage from the photomultiplier (typically about 100 mV) was balanced by the reference voltage. Following pulsed production via laser photolysis, the transient signal was read by the digitizer as the difference between the reference voltage and the actual signal. After each flash, the data from the transient analyzer were read by a computer and averaged into memory. Every 50 flashes, I_0 (the voltage from the photomultiplier before the flash) was read by a digital voltmeter. This I_0 value was then used to convert the transient voltage signal into a transient absorption. Computer-controlled mechanical relays were used to connect and disconnect the digital voltmeter to and from the signal lines during transient data acquisition. With this arrangement, we found that we could safely work with a transient absorbance change of 4×10^{-4}, corresponding to changes in the IO and I_2 concentrations of 4×10^{11} and 4×10^{12} cm^{-3}, respectively.

The cell was operated in continuous flow mode with gases regulated by calibrated mass flow controllers, and the total pressure was measured with a capacitance manometer. Reagent concentrations were calculated from the total pressure and the calibrated flows (except for I_2, which was measured by its light

absorption). Total flow rates of 5−900 cm^3 min^{-1} (STP) were used, sufficient to purge the cell contents between each laser pulse at a laser repetition rate of 0.3−1.0 Hz. This flow procedure prevented the accumulation of stable products (including condensation nuclei that could lead to aerosol formation) within the reaction zone. For the experimental conditions under which the results reported herein were obtained, no significant deposits which could effect transmission were observed on the cell windows. All experiments were performed at ambient temperature (295 ± 2 K).

Reactions were initiated by the laser flash photolysis of N_2O at 193 nm, in the presence of 60−600 Torr (8−80 kPa) of N_2.

$$N_2O + h\nu \rightarrow N_2 + O(^1D) \quad (12)$$

$$O(^1D) + N_2 \rightarrow O(^3P) + N_2 \quad (13)$$

The N_2 pressure was always in at least a 60-fold excess over that of N_2O to prevent complications from the reaction

$$O(^1D) + N_2O \rightarrow 2NO \quad (14)$$

In the presence of I_2, the oxygen atoms react to yield IO.

$$O(^3P) + I_2 \rightarrow IO + I \quad (15)$$

In the worst case, the amount of NO formed from reaction 14 was less than 10% of the amount of $O(^1D)$ quenched to $O(^3P)$. Thus, any possible complication from the IO + NO reaction (which is approximately one-fourth as fast as the IO + IO reaction) was minimized. This assessment is supported by our observation that there was no dependence of the kinetics on the N_2O concentration.

Data Analysis. Two different procedures were used for analyzing the data from the transient digitizer. In both cases, the data were treated by a nonlinear curve-fitting algorithm[15,16] to maximize the agreement (in a least-squares sense) between the calculated and measured curves. The first procedure, used for analyzing most of the IO decay curves, made use of the analytical formula for second-order decay of the radical light absorption:

$$A(t) = [1/A(0) + (2k/\sigma l)t]^{-1}$$

where $A(t) = \ln[I_0/I(t)]$ is the absorbance at time t; $A(0)$ the initial absorbance; k is the second-order rate coefficient; σ is the absorption cross section; and l is the optical path. This procedure was valid under conditions of relatively high I_2 concentration, where the rate of formation of IO was very fast compared to its rate of loss.

In the second procedure,[17] carried out primarily at lower I_2 concentrations, a model for the temporal behavior of the species being observed was written and used to derive the differential equations for the species concentrations. These equations were integrated with a fourth-order implicit Runge−Kutta algorithm.[18,19] The calculated IO and I_2 concentrations were transformed into digitizer readings and fit to the data holding chosen parameters constant. This procedure could be carried out on a single curve representing the temporal behavior at one wavelength or on two curves taken simultaneously at different wavelengths.

Results

Absorption Spectrum of IO. The absorption spectrum of IO over the spectral range 340−435 nm was determined by the flash photolysis of a mixture of 17 mTorr (2 Pa) I_2 and 1 Torr (133 Pa) N_2O in 200 Torr (27 kPa) N_2, with an IO concentration of about 1×10^{13} cm^{-3}. A few of the experiments were carried out with lower I_2 and N_2O concentrations and with IO concentrations of about $(2-3) \times 10^{12}$ cm^{-3}. At each wavelength, a decay curve was generated from an average of 100−150 individual experiments. Under the conditions of these experiments, the I_2 concentration is sufficiently high that there is no loss of IO due to reaction with O (see below), and the time to reach the peak absorbance was very short compared to the time scale for radical loss due to IO self-reaction. The peak absorbance, along with the simultaneously measured drop of I_2 absorption ($\sigma_{530\ nm} = 2.56 \times 10^{-18}$ cm^2),[20] provided absolute absorption cross sections for IO below 435 nm. Due to the interfering absorption from molecular iodine, relative absorbances were determined using CF_3I as IO radical source in the wavelength region 430−447 nm, however, and were scaled to the absolute measurements over the region of overlap. With the high-resolution grating in the Kratos monochromator, we could not carry out studies above 447 nm. Overlapping 20-nm-wide sections were scanned with 0.6-nm steps below and with 0.3-nm steps above 400 nm. Any 1-nm part of the spectrum contains two to seven points measured in two or more different runs. A total of 485 points were taken, which were then smoothed assuming a 0.3-nm Gaussian slit-function. Excellent reproducibility was observed, resulting in statistical uncertainties (2 standard deviations) of less than 20% in the absorption cross sections. For example, the value at the (4−0) band head at 427.2 nm was determined to be $(2.7 \pm 0.5) \times 10^{-17}$ cm^2. The resulting spectrum is presented in Figure 2.

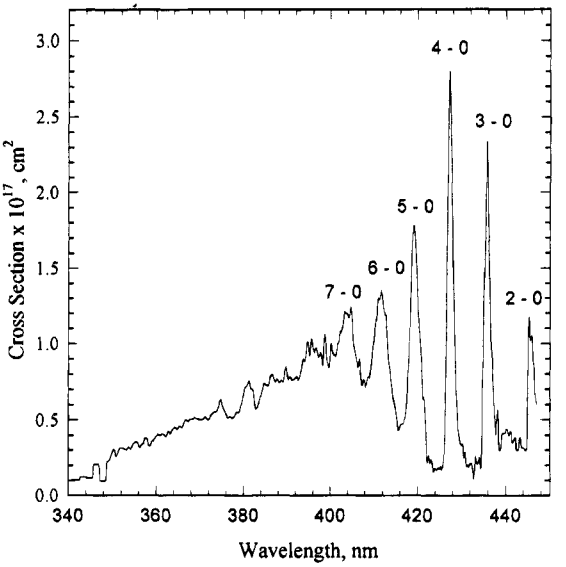

Figure 2. Absorption spectrum of the iodine monoxide radical taken at 0.3-nm resolution.

Kinetics of the Reactions O + I_2 and O + IO. To study reactions 8 and 15, experiments were performed with I_2 concentrations that were, on average, 1 order of magnitude less than those used for most of the spectral measurements. In the absence of N_2O, photolysis by 193-nm laser radiation leads to an immediate decrease in the absorption at 530 nm, due to the photolysis of I_2, followed by the very slow recombination of I atoms (Figure 3). With 3.2×10^{16} cm^{-3} N_2O added, an additional iodine loss can be observed from reaction 15. The IO absorbance, simultaneously monitored at 427.2 nm, shows a corresponding rise in the IO concentration. The reaction of atomic oxygen with iodine is in competition with the reaction of O with the product IO, reaction 8. By simultaneously monitoring the formation of IO and the loss of I_2, at relatively low I_2 concentrations (Figure 4), we have been able to obtain

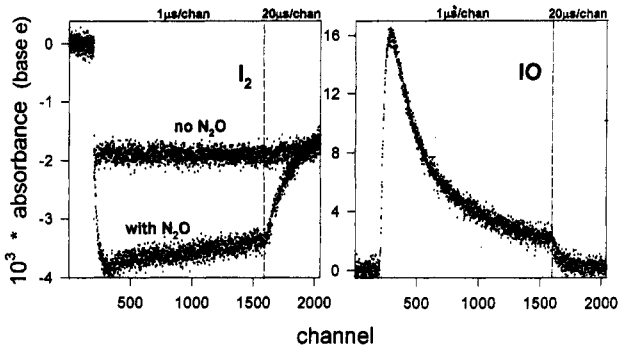

Figure 3. Temporal behavior of the absorption due to I_2 and to IO subsequent to the flash photolysis of a mixture of $I_2/N_2O/N_2$ at a high I_2 concentration and of a mixture containing no N_2O. The solid line through the IO data is the result of a second-order fit. A split time-base was used, and the data are shown plotted against channel number.

kinetic information on these reactions. The system was modeled with the following set of reactions:

$$O + I_2 \rightarrow IO + O \quad (15)$$

$$IO + O \rightarrow I + O_2 \quad (8)$$

$$IO + IO \rightarrow \text{products} \quad (9)$$

$$I + I \rightarrow I_2 \quad (16)$$

In the fitting procedure, the rate constants for reactions 15 and 8 were allowed to vary, the rate constant for reaction 9 was taken from the analysis described below, and the rate constant for reaction 16 was taken as 1.2×10^{-12} cm^3 s^{-1}, derived from a fit to the tail of the I_2 formation curve. The O(^{3}P) concentration was also fitted as a variable parameter. While the value for k_{16} has considerable uncertainty, and may also reflect an enhanced recombination rate in this complex system (see below), the values derived for k_8 and k_{15} were insensitive to the value of k_{16} over a range of over 1 order of magnitude. As a check on the validity of the fitted O(^{3}P) concentration and its effect on the rate constants, several experimental calibrations were conducted for some representative concentrations of N_2O and of laser energy. In these calibrations, I_2 was replaced with Br_2 to avoid halogen photolysis, and the [O(^{3}P)] was determined from the drop in the [Br_2] ($\sigma_{420nm} = 6.2 \times 10^{-19}$ cm^2).[20] These O(^{3}P) concentrations were statistically indistinguishable from the fitted values, as were the associated values of k_8 and k_{15}. From eight experiments (Table 1), we obtained $k_{15} = (1.4 \pm 0.4) \times 10^{-10}$ cm^3 s^{-1}, in excellent agreement with the previous measurement,[21] and $k_8 = (1.2 \pm 0.5) \times 10^{-10}$ cm^3 s^{-1}. The quoted uncertainty is twice the standard deviation and probably reflects mostly the uncertainty in the I_2 concentration measurements. The rate constant for the reaction of atomic oxygen with iodine monoxide is about 4 times greater that the rate constants for the comparable reactions of atomic oxygen with chlorine monoxide and with bromine monoxide.[22]

TABLE 1: Summary of IO + O(^{3}P) Experiments (Total Pressure 200 Torr)

I_2 (10^{13}/cm^3)	N_2O (10^{16}/cm^3)	O(^{3}P) (10^{13}/cm^3)	$k_{(I_2+O)}$ (10^{-10} cm^3/s)	$k_{(IO+O)}$ (10^{-10} cm^3/s)
2.1	3.0	3.1	1.6	0.9
2.4	4.6	2.9	1.4	1.2
3.4	1.9	1.9	1.5	1.5
3.5	8.0	5.0	1.7	1.3
6.9	11.8	8.9	1.2	0.9
6.7	6.1	4.8	1.4	1.1
4.6	5.1	3.7	1.5	1.6
3.2	1.9	1.5	1.2	1.3

Rate Constant for IO + IO. Rate constants for the self-reaction of IO were determined by simultaneously monitoring the absorption due to IO at 427.2 nm and that due to I_2 at 530 nm (Figure 3). For each experiment, the amount of I_2 consumed by reaction with O was determined and, hence, the amount of IO produced. From this, the absorption cross section was determined for that experiment. This allowed us to compensate for possible drifts in the monochromator setting. Second-order curve fitting of the IO decay, shown as the solid line in Figure 3, yielded $2k/\sigma l$. In these experiments, the I_2 concentration was kept above 1×10^{14} cm^{-3}. Under these conditions, O atoms

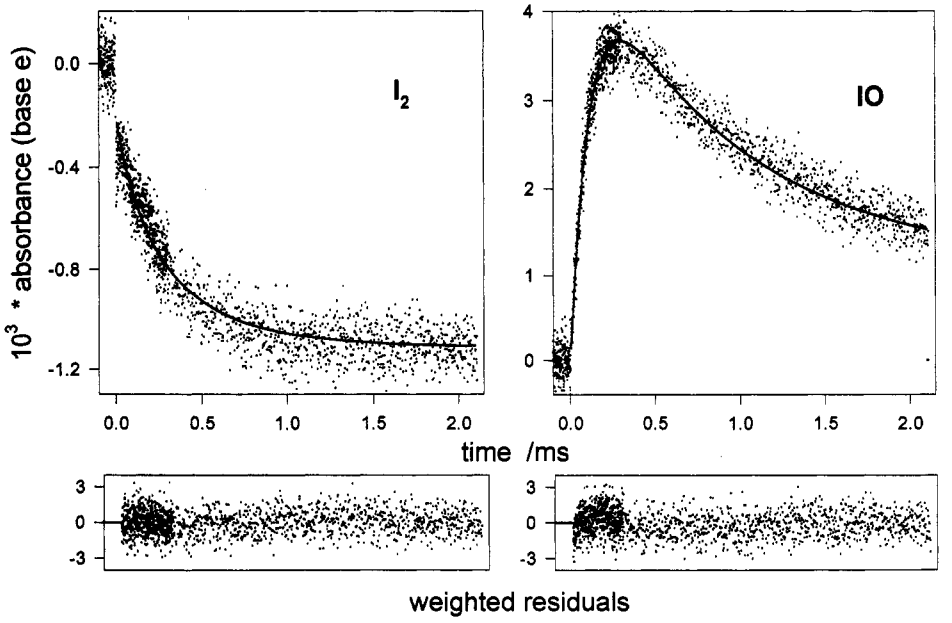

Figure 4. Temporal behavior of the absorption due to I_2 and to IO subsequent to the flash photolysis of a mixture of $I_2/N_2O/N_2$ at a low I_2 concentration. The solid lines are the fitted curves (see text). A split time-base was used, so that 40% of the data points were collected during the first 0.3 ms.

TABLE 2: Iodine Monoxide Radical Absorption Cross Section and Self-Reaction Rate, Measured at 200 Torr Total Pressure with Different I_2 and N_2O Concentrations

I_2 (10^{14} molecules/ cm^3)	N_2O (10^{15} molecules/ cm^3)	σ_{IO}(427.2nm) (10^{-17} cm^2)	k_{IO+IO} (10^{-11} cm^3 molecule^{-1} s^{-1})
1.3	2.3	2.7	7.9
2.1	32.4	2.4	7.9
2.3	50.2	2.8	9.1
2.6	1.9	3.4	7.1
3.0	1.9	3.2	9.3
3.9	49.9	2.9	8.4
4.2	25.9	2.6	8.6
5.1	2.9	2.5	8.0
5.3	64.8	2.7	7.6
6.5	2.6	2.8	6.5
8.3	4.5	2.9	7.0
9.8	4.9	1.9	6.8
13.8	6.8	2.8	7.0
14.3	9.4	2.9	9.2
14.3	19.1	3.2	8.7
14.3	34.0	2.6	7.0
average	2.8	7.9	
$2*\sigma$	0.5	1.9	

TABLE 3: IO Radical Absorption Cross Section and Self-Reaction Rate, Measured at Different Total Pressures

pressure (Torr)	I_2 (10^{14} molecules/ cm^3)	N_2O (10^{16} molecules/ cm^3)	σ_{IO}(427.2nm) (10^{-17} cm^2)	k_{IO+IO} (10^{-11} cm^3 molecule^{-1} s^{-1})
60	3.2	4.7	2.8	7.7
60	3.2	3.2	2.6	7.9
85	6.2	7.3	1.7	9.9
100	2.0	4.1	2.6	7.1
200 (av)	1.3−14.3	1.9−64.8	2.8	7.9
402	20.1	15.8	2.7	8.5
428	3.4	3.2	2.3	8.0
600	7.1	8.4	2.8	8.7
600	2.7	3.2	2.4	7.9
610	10.0	11.4	1.9	8.9

were depleted rapidly so that reaction 8 could be ignored and the temporal behavior of IO described by the two reactions.

$$O + I_2 \rightarrow IO + I \quad (15)$$

$$IO + IO \rightarrow \text{products} \quad (9)$$

Rate constants were measured at total pressures ranging from 60 to 600 Torr (8−80 kPa), I_2 concentrations between 1.4×10^{14} and 1.5×10^{15} cm^{-3}, and N_2O concentrations ranging from 2×10^{15} to 6.8×10^{16} cm^{-3} (Tables 2 and 3). The rate constant was found to be independent of these various parameters, and an average value of $k_9 = (8.0 \pm 1.7) \times 10^{-11}$ cm^3 s^{-1} was derived (the uncertainty being twice the standard deviation from 27 experiments).

Although the measured rate constant for IO decay did not depend on total pressure, the extent of reformation of I_2 did (Figure 5). The temporal behavior of I_2 lagged the decay of IO, indicating that the I_2 was not a primary product of the self-reaction of IO (reaction 9c). Rather, this behavior could be explained by a secondary reaction between iodine atoms and a product of the IO + IO reaction or from enhanced recombination of I atoms in this photochemical system. This conclusion is supported by the results of several experiments carried out with ICl as a radical source, where IO is generated without appreciable concentrations of I. Subsequent to the laser photolysis of a mixture of N_2O and ICl, no ClO absorption was

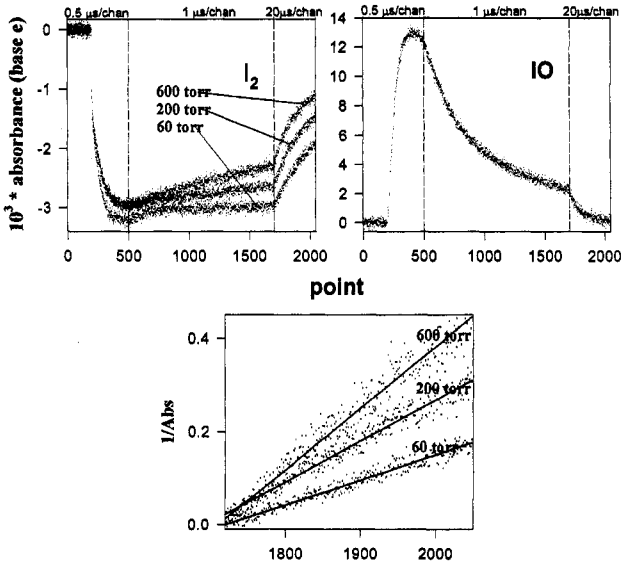

Figure 5. Temporal behavior of the absorption due to I_2 and to IO subsequent to the flash photolysis of a mixture of $I_2/N_2O/N_2$ at different total pressures, showing the pressure dependence of the I_2 re-formation and the lack of any pressure dependence in the IO decay. A second-order transform of the I_2 curves at long time indicate a second-order process.

detected at 265 nm, indicating that at least 90% of the reaction between O atoms and ICl occurs via

$$O + ICl \rightarrow IO + Cl \quad (17)$$

In this system, no I_2 formation was detected at 60, 200, or 600 Torr (8, 27, or 80 kPa) total pressure, supporting the conclusion that the self-reaction of IO is not a major direct source of I_2.

Studies of IO Loss with Other Radical Sources. We have also investigated the loss of IO produced by the flash photolysis at 193 nm of other reaction systems. In one set of experiments, CF_3I was used in place of I_2, with IO formed by the reaction

$$O + CF_3I \rightarrow CF_3 + IO \quad (18)$$

The overall decay rate of IO showed a strong correlation with the CF_3I concentration, with the apparent second-order rate constant increasing from 9×10^{-11} to 1.6×10^{-10} cm^3 s^{-1}. Experiments at the lower CF_3I concentrations and using the latter parts of the IO decay curve gave somewhat better (but never good) second-order fits. In addition to the more complex kinetic behavior, aerosol formation was also observed in this system. The addition of O_2 to the system, to scavenge the CF_3 radicals,

$$CF_3 + O_2 \rightarrow CF_3O_2 \quad (19)$$

led to serious deposit formation on the walls, slightly better second-order fits, and extremely high ($(2-4) \times 10^{-10}$ cm^3 s^{-1}) apparent second-order rate constants.

Experiments were also performed utilizing the photolysis of O_2 as a radical source, with the subsequent reaction of the atomic oxygen with I_2. The laser flash photolysis of a mixture containing 3.2×10^{14} cm^{-3} I_2 and 1.6×10^{18} cm^{-3} O_2 in 300 Torr (40 kPa) N_2 gave second-order IO decays, with a calculated rate coefficient of 5.4×10^{-11} cm^3 s^{-1}. When the I_2 concentration was halved and O_2 increased to 6.4×10^{18} cm^{-3}, the second-order rate constant for the IO decay dropped to 3.7×10^{-11} cm^3 s^{-1}. In both cases, excellent second-order fits were obtained. This dependence on O_2 and I_2 concentration (and hence on radical concentration) suggests complexity associated with secondary reactions, possibly associated with the ozone

formed in this system. Such complications may not always be discernible as deviations from second-order behavior. We decided not to probe further into these complications and to utilize only those results from the N_2O photolysis system for which there was no such inexplicable kinetic behavior and for which the results were more reproducible.

Discussion

The first spectral observation of the iodine monoxide radical in emission from a flame of methyl iodide was published by Vaidya.[23] Later, Durie observed six absorption bands[24] and performed an extensive analysis on the emission spectrum of the IO.[25] More recent work on the spectroscopy of this radical included high-resolution laser spectroscopy[26] and laser-induced fluorescence studies.[27] All of these authors agree that these spectral lines belong to the $A^2\Pi_{3/2} \leftarrow X^2\Pi_{3/2}$ electronic transition and that the $A^2\Pi_{3/2}$ state of iodine monoxide is predissociative.

There have been two prior reports of the absolute absorption spectra for the IO radical.[28,29] At the absorption maximum, the (4−0) band at 427.2 nm, these authors found $\sigma = 3.1(+2.0 -1.5) \times 10^{-17}$ cm^2 and $(3.1 \pm 0.6) \times 10^{-17}$ cm^2, respectively. In addition, there have been two other determinations of absolute cross section at the maximum, resulting in $\sigma = (2.2 \pm 0.5) \times 10^{-17}$ cm^2 [30] and $\sigma = (3.1 \pm 0.3) \times 10^{-17}$ cm^2.[11] Our value of $(2.7 \pm 0.5) \times 10^{-17}$ cm^2 is in quite good agreement with these previous measurements.

Over the spectral region 415−445 nm, our spectrum agrees well with that presented by Stickel et al.,[29] but the agreement with the spectrum presented by Cox and Coker[28] is somewhat poorer. The most significant difference is that we and Stickel et al. find the (2−0) peak to be significantly smaller than both (4−0) and (3−0) peaks, whereas Cox and Coker find the (2−0) peak about the same size as (3−0). In addition to the previously reported absorption of IO above 415 nm, we have identified two additional peaks at 411 and 403 nm, which we ascribe to the (6−0) and (7−0) transitions, respectively, and an underlying continuum starting around 420 nm and extending to about 350 nm.

This new spectrum for IO allows a recalculation of the rate at which IO is photolyzed in the troposphere. Assuming a constant 100% quantum efficiency for IO photodissociation, a photodissociation rate was calculated by summing the products of the averaged absorption cross section and the integrated solar flux over the entire spectrum. This integration-type calculation diminishes the differences arising from the small difference in spectral resolution. Average absorption cross sections and solar flux intensities[31] for a zenith angle of 40° are shown in the middle two columns of Table 4. As the spectral region above 447 nm was inaccessible with our monochromator, these numbers were taken from Cox and Coker.[28] The inclusion of absorption below 415 nm increases the rate of photodissociation from 0.18 to 0.28 s^{-1}. This photolysis rate means an atmospheric photolytic lifetime of 3.7 s at 40° solar zenith angle, considerably shorter than published values, and suggests that photolysis is the dominant loss process for IO during the daytime in the troposphere.

There are not reported experimental data for the reaction $O(^3P) + IO$ in the literature. Our value of 1.2×10^{-10} cm^3 s^{-1} is about 4 times greater than the estimated value.[22] This reaction is rate determining in the direct catalytic effect of iodine on ozone depletion in the upper stratosphere.

There have been several previous determinations of the rate constant for the self-reaction of IO: three by discharge-flow techniques and four by photolytic methods. The earliest work, employing discharge-flow with UV absorption detection of IO,

TABLE 4: Atmospheric Photolysis Rates of the IO Radical

wavelength region (nm)	average σ (10^{-18} cm^2)	actinic flux (10^{14} cm^{-2} s^{-1})	flux × σ (10^{-3} s^{-1})
345−350	1.5	7.4	1.1
350−355	2.9	8.5	2.4
355−360	3.3	7.9	2.6
360−365	3.7	8.8	3.3
365−370	4.2	10.8	4.5
370−375	4.9	9.8	4.8
375−380	3.8	11.0	4.2
380−385	5.6	9.2	5.1
385−390	6.0	10.1	6.0
390−395	6.7	10.5	7.0
395−400	7.6	12.8	9.7
400−405	7.8	15.3	11.9
405−410	9.4	17.3	16.2
410−415	9.3	18.3	17.0
415−420	11.1	18.6	20.7
420−425	8.3	18.3	15.2
425−430	11.4	18.4	21.0
430−435	6.1	19.0	11.6
435−440	11.7	19.0	22.3
400−445	3.0	22.1	6.6
445−450[a]	14.1	22.2	31.3
450−455[a]	4.0	25.1	10.0
455−460[a]	10.0	25.2	25.2
460−465[a]	4.2	25.8	10.8
465−470[a]	2.8	25.9	7.3

[a] Values taken from Cox and Coker.

yielded a rate constant of 2.6×10^{-12} cm^3 s^{-1},[32] much lower than that measured here or in other subsequent work. More recent work using a discharge-flow system with mass spectrometric detection has resulted in rate constants of 3.0×10^{-11} and 5.5×10^{-11} cm^3 s^{-1}.[33,34]

The photolytic studies include those in which IO was produced from the reaction of I with O_3 and those in which IO was produced by the reaction of O with I_2. If I is produced in the self-reaction of IO, then regeneration of IO would affect the results in those experiments where O_3 is present. In the earliest photolytic study, I was produced by the modulated photolysis of CH_3I.[28] A considerable amount of aerosol was observed, and a very high rate constant was reported, $k = 4.0 \times 10^{-10}$ cm^3 s^{-1}. In subsequent work from the same laboratory, in which IO was produced by the photolysis of I_2 in the presence of O_3, a lower rate constant was measured, but the reaction was observed to have both first- and second-order components, with the second-order component having pressure independent and pressure dependent parts.[30]

The most thorough study of the self-reaction of IO involved the use of both the flash photolysis of I_2 in the presence of O_3 and the flash photolysis of O_2 in the presence of I_2.[11] The apparent rate constant obtained from the $I + O_3$ system exhibited a pressure dependence, increasing from 3.1×10^{-11} to 4.6×10^{-11} cm^3 s^{-1} as the pressure was raised from 21 to 650 Torr (2.8 to 87 kPa) with Ar, while the rate constant from the $O + I_2$ system exhibited no pressure dependence. This suggests a pressure dependence in the branching ratio to produce I atoms, but no pressure dependence on the overall rate constant. The room temperature rate constant obtained in that work, $k = 5.6 \times 10^{-11}$ cm^3 s^{-1}, is somewhat lower than that obtained here when N_2O was used as the oxygen atom source, but similar to the value we obtained in the more complex reaction system where O_2 was used as the source.

In a study involving the laser flash photolysis of I_2 in the presence of O_3 and laser absorption spectroscopy for the detection of IO, a rate constant of 6.6×10^{-11} cm^3 s^{-1} was obtained at a total pressure of 1 atm.[29] While this rate constant

is slightly lower than that measured in the present work ($k = 8.0 \times 10^{-11}$ cm^3 s^{-1}), the difference is not statistically significant.

Acknowledgment. This work was supported in part by the United States Air Force through Contract 89CS8204 and the United States Army through MIPR M-G-164-93. Ongoing support for this laboratory is also received from NASA's Upper Atmosphere Research Program. We thank Dr. Andrzej W. Miziolek for help and for useful discussions.

References and Notes

(1) Zafiriou, O. C. *J. Geophys. Res.* **1974**, *79*, 2730.
(2) Chameides, W. L.; Davis, D. D. *J. Geophys. Res.* **1980**, *85*, 7383.
(3) Chatfield, R. B.; Crutzen, P. J. *J. Geophys. Res.* **1990**, *95*, 22319.
(4) Jenkin, M. E.; Cox, R. A.; Candeland, D. E. *J. Atmos. Chem.* **1985**, *2*, 359.
(5) Barnes, I.; Bonsang, B.; Brauers, T.; Carlier, P.; Cox, R. A.; Dorn, H. P.; Jenkin, M. E.; Le Bras, G.; Platt, U. Air Pollution Research Report. OCENO-NOX-CEC Project; 1991.
(6) Jenkin, M. E. *A comparative assessment of the role of iodine photochemistry in tropospheric ozone depletion*; Jenkin, M. E., Ed.; NATO-ASI series no. 17; Springer-Verlag: Berlin, 1993.
(7) Wayne, R. P. *The chemistry of atmospheres*; Clarendon Press: Oxford, 1991.
(8) Solomon, S.; Burkholder, J. B.; Ravishankara, A. R.; Garcia, R. R. *J. Geophys. Res.* **1994**, *99*, 20929.
(9) Solomon, S.; Garcia, R. R.; Ravishankara, A. R. *J. Geophys. Res.* **1994**, *99*, 20491.
(10) Buben, S. N.; Trofimova, E. M.; Spassky, A. I.; Messineva, N. A. Study of atmospheric reactions of IO radicals. Report B. Reaction of iodine monoxide with ozone. The Institute of Energy Problems of Chemical Physics, Russian Academy of Sciences, 1994.
(11) Sander, S. P. *J. Phys. Chem.* **1986**, *90*, 2194.
(12) Stein, S. E.; Rukkers, J. M.; Brown, R. M. *Structures & Properties*; 1.2 ed.; Stein, S. E., Rukkers, J. M., Brown, R. M., Eds.; NIST: Gaithersburg, MD, 1991.
(13) Huie, R. E.; Laszlo, B. In Halon Replacements: Technology and Science. *Advances in Chemistry Series*, in press.
(14) The identification of commercial equipment and materials is only to describe completely the system and does not imply recognition of endorsement by the National Institute of Standards and Technology, nor does it imply that the equipment or material identified are necessarily the best available for the purpose.
(15) Bevington, P. B. *Data reduction and error analysis for the physical sciences*; McGraw-Hill: New York, 1969.
(16) Marquardt, D. W. *J. Soc. Ind. Appl. Math.* **1963**, *11*, 431.
(17) Laszlo, B. Manuscript in preparation.
(18) Gottwald, B. A.; Wanner, G. *Computing* **1981**, *26*, 355.
(19) Gottwald, B. A.; Wanner, G. *Simulation* **1982**, *37*, 169.
(20) Calvert, J. G.; Pitts, J. N. *Photochemistry*; John Wiley & Sons: New York, 1966.
(21) Ray, G. W.; Watson, R. T. *J. Phys. Chem.* **1981**, *85*, 2955.
(22) Atkinson, R.; Baulch, D. L.; Cox, R. A.; Hampson, R. F.; Kerr, J. A.; Troe, J. *J. Phys. Chem. Ref. Data* **1992**, *21*, 1125.
(23) Vaidya, W. M. *Proc. Indian Acad. Sci. Sect. A* **1937**, *6*, 122.
(24) Durie, R. A.; Ramsay, D. A. *Can. J. Phys.* **1958**, *36*, 35.
(25) Durie, R. A.; Legay, F.; Ramsay, D. A. *Can. J. Chem.* **1960**, *38*, 444.
(26) Bekooy, J. P.; Meerts, W. L.; Dymanus, A. *J. Mol. Spectrosc.* **1983**, *102*, 320.
(27) Inoue, G.; Suzuki, M.; Washida, N. *J. Chem. Phys.* **1983**, *79*, 4730.
(28) Cox, R. A.; Coker, G. B. *J. Phys. Chem.* **1983**, *87*, 4478.
(29) Stickel, R. E.; Hynes, A. J.; Bradshaw, J. D.; Chameides, W. L.; Davis, D. D. *J. Phys. Chem.* **1988**, *92*, 1862.
(30) Jenkin, M. E.; Cox, R. A. *J. Phys. Chem.* **1985**, *89*, 192.
(31) Finlayson-Pitts, B. J.; Pitts, J. N. *Atmospheric Chemistry*; John Wiley & Sons: New York, 1986.
(32) Clyne, M. A. A.; Cruse, H. W. *Trans. Faraday Soc.* **1970**, *66*, 2227.
(33) Martin, D.; Jourdain, J. L.; Laverdet, G.; Le Bras, G. *Int. J. Chem. Kinet.* **1987**, *19*, 503.
(34) Barnes, I.; Bastian, V.; Becker, K. H.; Overath, R. D. *Int. J. Chem. Kinet.* **1991**, *23*, 579.

JP950628+